2023 7th International Symposium on Instrumentation Systems, Circuits and Transducers (INSCIT) | 979-8-3503-2651-2/23/$31.00 ©2023 IEEE | DOI: 10.1109/INSCIT59673.2023.10258500

Current Transformer-Based System for Measuring Leakage Current

Stéphane Carvalho*, Graziella Bedenik*, Lucas Molina*, Elyson Ádan Nunes Carvalho*,
Ulisses D. E. S. Lebre†, and Charles A. C. de Araujo†
*INESC P&D Brasil and Electrical Engineering Department, Federal University of Sergipe, São Cristóvão, Brazil
s.stephanecarvalho@gmail.com, graziella.bedenik@gmail.com, lmolina@academico.ufs.br, ecarvalho@academico.ufs.br
†Eneva, Rio de Janeiro, Brazil
ulisses.lebre@eneva.com.br, charles.cordeiro@eneva.com.br

***Abstract*—Insulators are crucial components in high-voltage electrical systems, and their failure can result in substantial economic losses exceeding acquisition and installation costs. Failures can also overload transmission lines and cause power outages in large areas. Pollution, particularly in coastal regions, is a leading cause of insulator failure. Soluble salts like $NaCl$ and Na_2SO_4 adhere to the insulator surface, creating an alternative conductive path for current leakage. In this work, a current transformer was used to develop a measurement system. The system underwent core characterization experiments and signal post-processing. The constructed prototype successfully measured and recovered the signal, demonstrating its suitability and viability for measuring leakage current in insulators. The system is capable of measuring currents ranging from hundreds of microamperes to tens of milliamperes within the frequency range of 60 Hz to 540 Hz. It enables continuous monitoring and analysis of the current in insulators.**

***Index Terms*—leakage current, current transformer, magnetic measurement**

I. Introduction

Insulators are crucial components of high-voltage electrical systems, serving as both mechanical support and electrical insulation [1]–[5]. Failures associated with these elements can result in significant economic losses, as well as power supply disruptions in large areas, and even the destruction of the entire insulator [1], [2], [5]. Such outcomes may come from mechanical or environmental factors, and the effect is magnified in coastal areas with the deposition of soluble salts, like $NaCl$ and Na_2SO_4, on their surfaces, creating a conductive path that causes current leakage [2], [3], [6], [7].

Leakage currents can be measured using shunt resistors, optical sensors, Hall effect sensors, and Current Transformers (CTs). Among these techniques, CTs are commonly used for leakage current measurement. However, there is a lack of studies that characterize this type of sensor and investigate its application in measuring low currents, creating a significant knowledge gap in the field of CTs for current measurement [7]–[9].

This work was developed as part of the project "GImpSI - Gestão dos Impactos da Salinidade em Isolamentos", with Eneva S.A. and INESC P&D Brasil. It was financed in part by the R&D Program of the Brazilian Electricity Regulatory Agency, code PD-11278-0001-2021, and in part by the Brazilian Coordination for the Improvement of Higher Education Personnel (CAPES) - Finance Code 001.

Therefore, this work proposes a CT-based system for measuring leakage currents in high-voltage insulators, enabling continuous monitoring and analysis. It covers a current range of hundreds of microamperes to tens of milliamperes, with a frequency range of 60 Hz to 540 Hz (ninth harmonic). The system's specifications were tailored to meet the requirements of the UTEPS I electric power substation in Barra dos Coqueiros, Sergipe, Brazil. Additionally, this work contributes to both technological advancements in leakage current sensors and scientific research. It investigates and analyzes the electrical model of the sensor and the chosen measurement technique. Notably, it provides a methodology for characterizing the specifications of the CT, filling a crucial gap in the existing literature. This paper is organized as follows. Section II discusses the related work found in the literature. The experiments descriptions are presented in Section III, followed by the obtained results and their discussion, shown in Section IV. Conclusions and future work are presented in Section V.

II. Related Works

Real-time monitoring of insulation degradation has been extensively researched in recent years, with many studies evaluating leakage current sensing techniques dating back to the 1990s [7], [10]. The goal of developing these systems is to optimize preventive maintenance on insulation, resulting in resource savings and preventing accidents [3], [6], [11], [12].

One of the earliest studies on leakage current characteristics in insulators for preventive maintenance was conducted by Fierro et al. [7] and Ramirez et al. [10]. They carried out laboratory tests to investigate the behavior of leakage current under various conditions of pollutant deposition and types of insulators. They proposed a method for real-world applications using a current transformer with a core of high magnetic permeability as the sensing element. Additionally, they presented a predictability analysis to enhance preventive maintenance from the beginning of the insulation installation.

Shunt resistor measurement has been used in several studies, such as [13], [14], and [11], to assess new and naturally polluted insulators. The analysis of the results indicates a significant correlation between the waveform and total harmonic distortion of the leakage current signal and the natural

degradation of the insulator. Other works have also used the harmonics of the leakage current signal to determine insulator degradation, including [15], [16], [1], [17], [12], [18], [19], and [20].

Several studies have explored alternative methods for measuring leakage current, such as optical fiber sensors, as demonstrated in [6], [9], and [2]. Optical fiber sensors offer good immunity to magnetic effects, which is a significant challenge in low-magnitude electrical measurements when high voltages are present.

In [12], the authors introduce a monitoring system utilizing a current transformer as the sensing element, similar to the approach described in [7]. The main advantage of this system is its ability to measure without direct contact with the insulator chain, thereby preserving its integrity. The sensing element comprises a supermalloy core with significantly higher magnetic permeability compared to traditional ferrite or iron powder cores. However, there is still a gap in the literature regarding the characterization of CTs, specifically in terms of adequacy of the sensor's suitability for desired specifications and investigating its performance in measuring low-magnitude currents.

III. Experiments Descriptions

Three experiments were conducted during the development of this work. They characterized the core for the sensor construction, investigated the measurement range, and acquired and reconstructed the current signal. These crucial steps enabled the development of a sensor capable of assessing high-voltage insulator quality by coupling it to the grounding wire of the insulator.

These experiments will be described as follows in Subsections III-A, III-B, and III-C.

A. Shape and size of the core

Characterization experiments were performed using two nanocrystalline cores. The goal was to obtain information about the core's magnetic permeability and inductance and to investigate the shape and size of the core that best met the design specifications.

For this purpose, we first tried to find the relationship between core permeability and frequency substituting $\mathfrak{R} = {}^{l}/_{\mu A}$ (where $\mathfrak{R}$ is the reluctance in H^{-1}, l is the length of the magnetic path in m and A is the cross-sectional area of the material in m^2) and $\mathfrak{F} = NI$ (where $\mathfrak{F}$ is the magnetomotive force, N the number of turns and I the current) in the magnetic flux equation $\Phi = {}^{\mathfrak{F}}/_{\mathfrak{R}}$, obtaining

$$\Phi = \frac{\mu N A I(t)}{l}, \tag{1}$$

where only the permeability, μ, is unknown. Using Faraday's law, we get that the voltage across the coil is given by

$$V_N(t) = N\frac{\mathrm{d}\Phi}{\mathrm{d}t} \Rightarrow \frac{\mathrm{d}\Phi}{\mathrm{d}t} = \frac{V_N(t)}{N}, \tag{2}$$

that could be reorganized as:

$$\Phi = \frac{1}{N}\int V_N(t)\,\mathrm{d}t. \tag{3}$$

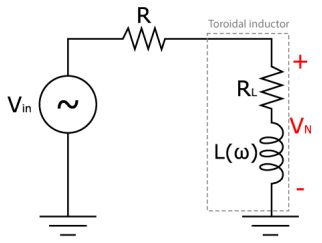

Fig. 1: Circuit used for experimental measurement of inductance and magnetic permeability as a function of frequency.

From (1) and (3) we obtain:

$$\frac{\mu N A I(t)}{l} = \frac{1}{N}\int V_N(t)\,\mathrm{d}t. \tag{4}$$

By applying the derivative on both sides of (4) and performing some algebraic manipulations, it is possible to write the voltage across the coil surrounding the core as a function of the applied current as

$$V_N(t) = \frac{\mu A N^2}{l}\,\frac{\mathrm{d}I(t)}{\mathrm{d}t}. \tag{5}$$

The wiring diagram shown in Fig. 1 was considered to make the experimental measurement of inductance L and consequently use this value to find the permeability at L terminals, μ_N. The voltage V_N, also taken at the inductor terminals, can be modeled as the voltage between the inductance L, which, by hypothesis, varies as a function of frequency ω, in series with an intrinsic resistance R_L, measured across the winding. Hence, it is possible to obtain several points of V_N *versus* f, allowing us to experimentally reach magnetic permeability and inductance values of the CT.

Analyzing the voltage divider in the circuit in question, we have that

$$\left|\frac{sL + R_L}{sL + R_L + R}\right| = G, \tag{6}$$

where G indicates the gain, which can vary. We can rewrite equation (6) for this gain by isolating L and as a function of R and f, obtaining:

$$L = \frac{\sqrt{R^2 + 2RR_L + (1 - G^2)R_L}}{2\pi f\sqrt{G^2 - 1}}, \tag{7}$$

Based on this equation, we choose different values of resistance and frequency in order to find the gain of the system equal to G. With the pairs (w, R) found, we calculate the inductance L associated with each of the frequencies.

For this characterization, we used two non-bipartite toroidal cores from the manufacturer Magmattec. Both cores were made of the same material and had the same number of turns ($N = 1000$), but they differed in dimensions. Core 1, model MMT521T82.46.35B, had a height of 35 mm, inner radius of 23 mm, and outer radius of 41 mm. Core 2, model MMT521T50.40.20B, had a height of 20 mm, inner radius of 20 mm, and outer radius of 25 mm. Both cores can be seen in Fig. 2. By comparing the response obtained from

Fig. 2: Cores with 1000 turns used in characterization tests.

these two cores, we could determine which one best suited the specifications of the sensor design.

B. Measurement range and information quality

From the choice of core dimensions, the second experiment consisted in perform tests to investigate the relationship between measurement range and information quality with the amount of CT turns. To this end, one hundred and fifty turns ($N = 100$ and $N = 50$) were made on two other core units chosen from the first experiment and we studied their frequency responses.

We also performed experiments using a bipartite core with the same dimensions. This one was coiled with eighty-eight coils ($N = 88$). From these tests, it was possible to define the shape of the core to be used (bipartite or non-bipartite) and the number of turns.

C. Reconstruction experiments

After performing the aforementioned characterization experiments, we have to process the measured signal to reconstruct the original current signal, validating the measurement of leakage current in insulators.

This processing stage assumes the linearity of the system and employs mathematical models for both the input and output signals. Specifically, a sum of sinusoids and linear regression is utilized. This step serves as a means to validate the leakage current measurement using the developed prototype in this work.

The subsequent section, Section IV, will present the results and analysis obtained from the conducted experiments.

IV. Results and Discussion

This section presents the results obtained from the experiments performed for the development of the system for measuring leakage current in insulators proposed in this work. They are organized into subsections, according to the intended purpose of each one, for a better understanding and fluidity of the discussions.

A. Shape and size of the core

From the characterization experiments performed, it was possible to obtain information on the inductance of the CT

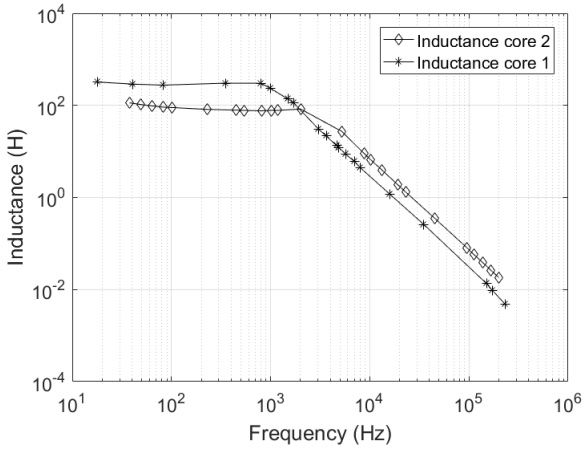

Fig. 3: Estimated inductance from cores 1 and 2 with 1000 turns.

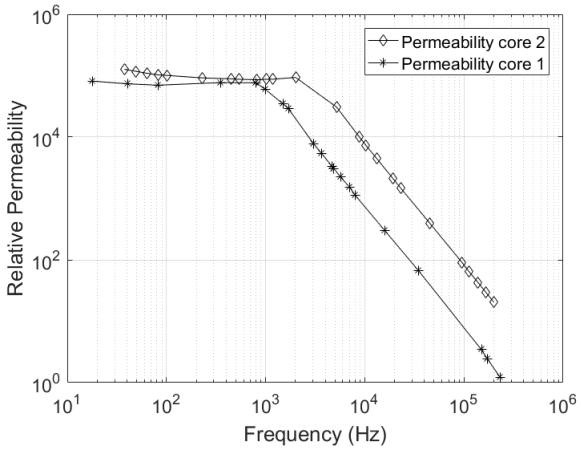

Fig. 4: Estimated permeability from cores 1 and 2 with 1000 turns.

and permeability of the cores. Such results can be visualized in figures 3 e 4.

From these figures, we can observe a satisfactory performance in the frequencies of interest (60 Hz to 540 Hz) for both cores, as the inductance remains approximately constant within this range. Furthermore, despite the notable difference in inductance, the relative magnetic permeability is similar for both cores within this frequency range. However, core one offers better information quality and easier measurement due to its significantly higher inductance in the region of interest. Based on this result, we selected the core one for sensor development.

B. Measurement range and information quality

Proceeding to the experiments that aimed to investigate the relationship of measurement range and quality with the number of CT turns, we obtained the frequency response (Bode) plots for four different CTs. In the Fig. 5 the result can be seen for the core with 1000, 100 and 50 turns with a

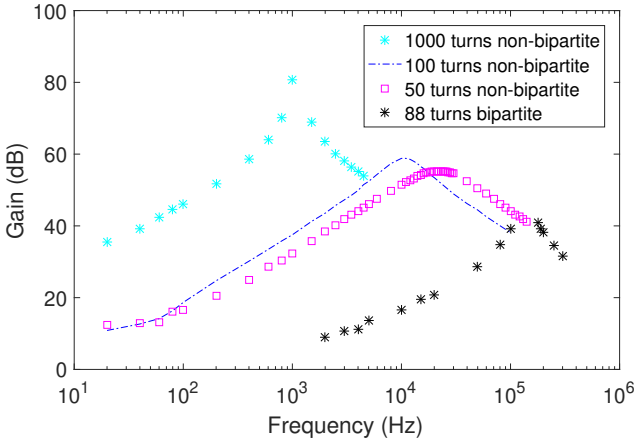

Fig. 5: Frequency response obtained for the cores with 1000, 100 e 50 turns non-bipartite and 88 turns with a bipartite core, where the gain in dB is the result of applying a 7 mA current in the primary by the measured voltage in the secondary.

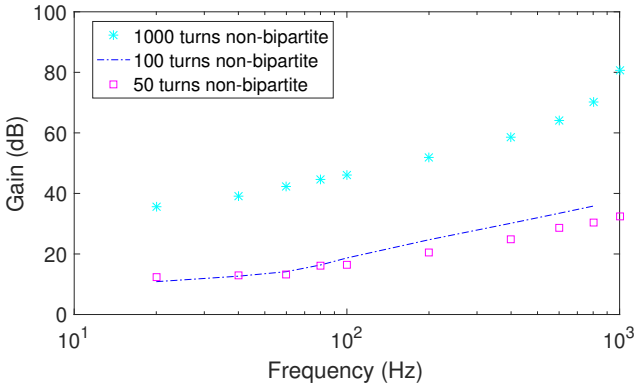

Fig. 6: Frequency response obtained for the cores with 1000, 100 e 50 turns non-bipartite in the frequency range of interest, where the gain in dB is the result of applying a 7 mA current in the primary by the measured voltage in the secondary.

non-bipartite core and also for a bipartite core with 88 turns, respectively, where the gain in dB is a result of the application of the current in the primary by the measured voltage in the secondary of the CT.

After analyzing the responses, it was observed that the bipartite core did not perform measurements within the desired frequency range, unlike the other cores, as shown in Fig. 6. However, the one with 1000 turns had a sharp gain in the frequency range of interest, which can hinder the reconstruction of the measured signal. The core with 100 turns exhibited higher gains and lower sensitivity to low-frequency noise than the core with 50 turns, as well as advantages in terms of cost, reproducibility, and gain compared to the one with 1000 turns. Therefore, the non-bipartite core with 100 turns was selected as the sensor for developing the leakage current measurement system.

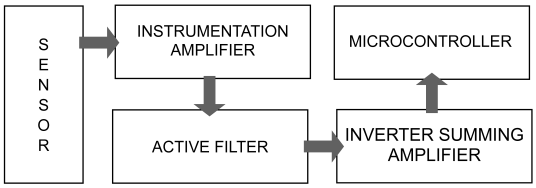

Fig. 7: Block diagram of the developed signal conditioning system.

C. Description of the acquisition circuit and signal digital reconstruction

To acquire the measured signal, we implemented the conditioning circuit described in the block diagram in Fig. 7. In this, the sensor is the CT built; the instrumentation amplifier aims to reduce the common mode voltage and the noise at low frequencies; the active filter aims to reduce noise at high frequencies and prevent signal clipping at high frequencies; and the inverter summing amplifier was implemented to guarantee the analog input voltage limits for a microcontroller (0 to 3.3 V). The complete wiring diagram of the designed conditioner circuit is shown in Fig. 8.

A PCB was made from the circuit and used for testing the complete measurement system, including current measurement with the CT and output of the signal conditioner. To generate test signals with known harmonic components, a function generator capable of loading and retrieving arbitrary signals directly from/to the computer was used.

Since the sensing element exhibits varying gains in the frequency range of interest (60 to 540 Hz), as depicted in Fig. 6, the measured signal is distorted due to different amplifications in each different frequency of the current signal. To demonstrate the aforementioned distortion, we conducted an experiment to measure a current periodic signal with harmonic components ranging from 60 Hz to 540 Hz. The resulting current signal and the corresponding voltage measured by the sensor can be observed in Fig. 9, revealing a noticeable disparity between the output and input signals.

Despite their dissimilarities, it is possible to reconstruct the original signal by compensating for the distortions caused by the frequency response of the sensor. This compensation process involves two essential steps: determining the sensor's gain for the measured frequency components and calculating the magnitude of these frequency components in the output signal.

The first step, which involves determining the sensor's gain for the measured frequency components, has already been completed in section IV-B. Now, the remaining task is to extract the gains from the bode diagram depicted in Fig. 6.

The second step involves recovering the Fourier series coefficients of the output signal. This can be achieved through linear numerical regression, using:

$$a + \sum_{i=1}^{i=9} b_i \cdot cos(n \cdot 2\pi \cdot 60 \cdot t) + c_i \cdot cos(n \cdot 2\pi \cdot 60 \cdot t) \quad (8)$$

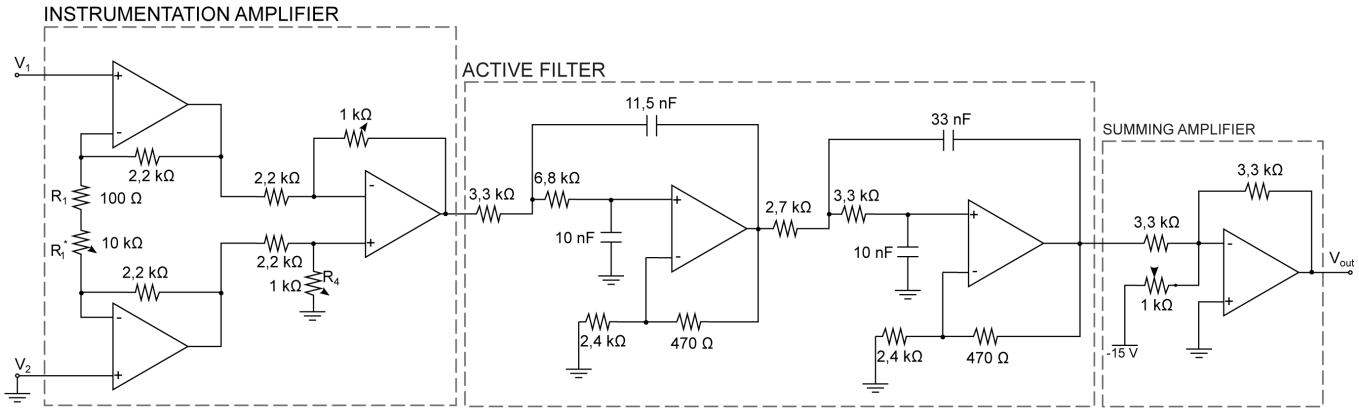

Fig. 8: Designed and implemented signal conditioner. Here, V_1 and V_2 are the two outputs of the developed CT and V_{out} is the final output of the measurement system.

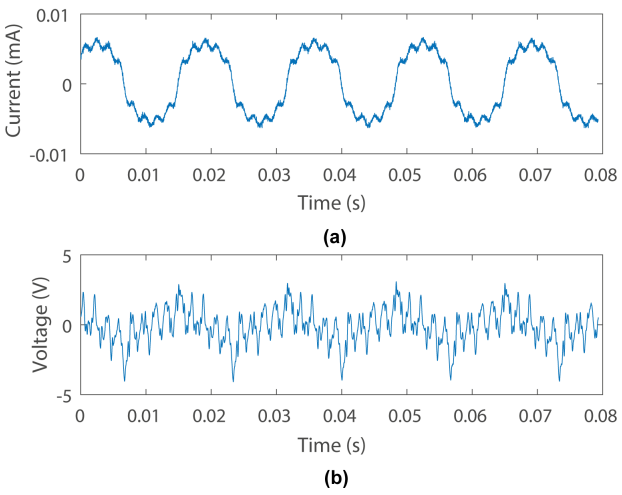

Fig. 9: (a) Signal with different magnitudes at each harmonic of interest, generated to simulate leakage current in insulators; (b) Voltage obtained at the output of the measurement circuit, before post-processing.

as the model equation, where a, b_i and c_i are parameters of the equation. Fig. 10 shows the voltage signal measured at the sensor output along with the signal obtained from the regression model (Eq. (8)).

Once the output signal has been modeled by Eq. (8), we can calculate the magnitudes of its frequency components using

$$M_i = \sqrt{b_i^2 + c_i^2}, \tag{9}$$

where M_i is the magnitude of the *ith* harmonic frequency.

After calculating the magnitudes, we multiply them by the inverse of the sensor gain at each frequency to obtain the measurement for the original signal at the input of the sensor.

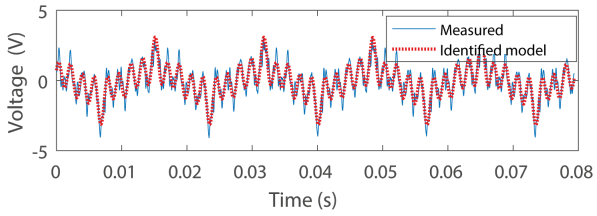

Fig. 10: Output signal of the measurement circuit from the identified model.

The resulting signal is depicted in Fig. 11, where we observe that, despite a phase difference, the measured signal after this process is in agreement with the original signal used to simulate the insulator leakage current at the sensor input.

This result is emphasized through the dispersion analysis performed using fifty samples of the output signal for the same input signal. Such distribution analysis resulted in Table I, where it is possible to notice a higher dispersion only at the fundamental frequency of 60 Hz, caused by the noise inherent to the electrical network coupled to the system and a high agreement between the input and the reconstructed outputs at the other frequencies.

V. Conclusion

This paper proposes a system for measuring leakage current in high-voltage insulators. The prototype accurately measures and recovers the signal, indicating its reliability as a method. The experiments involved current signals ranging from a few hundred microamperes to tens of milliamperes, with a fundamental frequency of 60 Hz and nine harmonics up to 540 Hz.

The results demonstrate that a core with 100 coils can linearly measure such currents. Comparative analysis confirms that the developed system exhibits low dispersion at

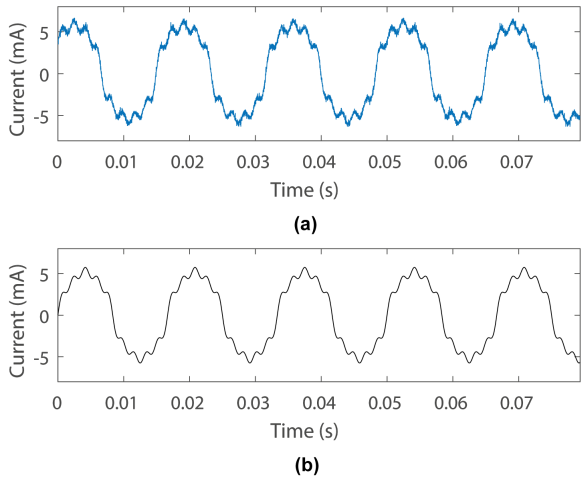

Fig. 11: (a) Reference current signal simulating the leakage current in the insulator; (b) Current signal reconstructed with data from the measurement circuit output, after post-processing.

TABLE I: Comparative analysis between the signal simulating the current in the insulator and the reconstructed output of the developed system for fifty measurements. The frequency is presented in Hz while the other metrics are presented in mA.

f	Real Magnitude	Error Mean	Standard Deviation
60	6	$0.4771E^{-4}$	0.1573
180	0.7	$0.1749E^{-4}$	0.0126
300	0.3	$0.1050E^{-4}$	0.0048
420	0.2	$0.1120E^{-4}$	0.0039
540	0.7	$0.0501E^{-4}$	0.0044

the frequencies of interest. Consequently, this meter enables accurate measurement and recovery of leakage current in insulators without system interference. In addition, this paper introduces a characterization methodology for CTs to match them with desired signal specifications. This is crucial due to the dynamic characteristics of CTs, which can result in differences between input and output signals, especially with multiple frequency components. By filling this gap in the literature, we address an important aspect of CT performance and enhance understanding in this field.

Since the sensor is in its final development stage, high-voltage tests have not been conducted yet. Future work will involve conducting these tests, comparing the results obtained with other techniques, and exploring methods to improve the constancy of sensor gain at the frequencies of interest. This improvement aims to enhance signal quality and streamline data reconstruction in the processing phase.

REFERENCES

[1] A. A. Salem, R. Abd-Rahman, S. A. Al-Gailani, M. S. Kamarudin, H. Ahmad, and Z. Salam, "The leakage current components as a diagnostic tool to estimate contamination level on high voltage insulators," *IEEE Access*, vol. 8, pp. 92 514–92 528, 2020.

[2] M. M. Werneck, D. M. dos Santos, C. C. de Carvalho, F. V. B. de Nazaré, and R. C. d. S. B. Allil, "Detection and monitoring of leakage currents in power transmission insulators," *IEEE sensors journal*, vol. 15, no. 3, pp. 1338–1346, 2014.

[3] M. Akbar, R. Ullah, and S. Alam, "Aging of silicone rubber-based composite insulators under multi-stressed conditions: an overview," *Materials Research Express*, vol. 6, no. 10, p. 102003, 2019.

[4] K. F. Portella, F. Piazza, P. C. Inone, S. Ribeiro Jr, M. S. Cabussú, D. P. Cerqueira, and C. S. d. S. Chaves, "Efeitos da poluição atmosférica (litorânea e industrial) em isoladores da rede elétrica da região metropolitana de salvador," *Química Nova*, vol. 31, pp. 340–348, 2008.

[5] B. Dolník, L. Šárpataky, I. Kolcunová, and P. Havran, "Sensing method using multiple quantities for diagnostic of insulators in different ambient conditions," *Sensors*, vol. 22, no. 4, p. 1376, 2022.

[6] S. C. Oliveira, E. Fontana, F. J. d. M. de Melo *et al.*, "Leakage current activity on glass-type insulators of overhead transmission lines in the northeast region of brazil," *IEEE Transactions on Power Delivery*, vol. 24, no. 2, pp. 822–827, 2009.

[7] J. Fierro-Chavez, I. Ramirez-Vazquez, and G. Montoya-Tena, "On-line leakage current monitoring of 400 kv insulator strings in polluted areas," *IEE Proceedings-Generation, Transmission and Distribution*, vol. 143, no. 6, pp. 560–564, 1996.

[8] T. d. C. BATISTA *et al.*, "Transformadores de corrente com núcleo de liga nanocristalina utilizados para serviços de medição e proteção em sistemas elétricos." 2014.

[9] E. Fontana, S. C. Oliveira, F. J. M. M. Cavalcanti, R. B. Lima, J. F. Martins-Filho, and E. Meneses-Pacheco, "Novel sensor system for leakage current detection on insulator strings of overhead transmission lines," *IEEE transactions on power delivery*, vol. 21, no. 4, pp. 2064–2070, 2006.

[10] I. Ramirez-Vazquez and J. L. Fierro-Chavez, "Criteria for the diagnostic of polluted ceramic insulators based on the leakage current monitoring technique," in *1999 Annual report conference on electrical insulation and dielectric phenomena (Cat. No. 99CH36319)*, vol. 2. IEEE, 1999, pp. 715–718.

[11] N. Bashir and H. Ahmad, "Odd harmonics and third to fifth harmonic ratios of leakage currents as diagnostic tools to study the ageing of glass insulators," *IEEE Transactions on Dielectrics and Electrical Insulation*, vol. 17, no. 3, pp. 819–832, 2010.

[12] R. J. Villalobos, L. A. Moran, F. Huenupán, F. Vallejos, R. Moncada, and C. Pesce, "A new current transducer for on-line monitoring of leakage current on hv insulator strings," *IEEE Access*, vol. 10, pp. 78 818–78 826, 2022.

[13] H. Ahmad, M. Salam, L. Y. Ying, and N. Bashir, "Harmonic components of leakage current as a diagnostic tool to study the aging of insulators," *Journal of Electrostatics*, vol. 66, no. 3-4, pp. 156–164, 2008.

[14] A. H. El-Hag, A. N. Jahromi, and M. Sanaye-Pasand, "Prediction of leakage current of non-ceramic insulators in early aging period," *Electric power systems research*, vol. 78, no. 10, pp. 1686–1692, 2008.

[15] R. Ghosh, B. Chatterjee, and S. Chakravorti, "A novel leakage current index for the field monitoring of overhead insulators under harmonic voltage," *IEEE Transactions on Industrial Electronics*, vol. 65, no. 2, pp. 1568–1576, 2017.

[16] D. Maadjoudj, A. Mekhaldi, and M. Teguar, "Flashover process and leakage current characteristics of insulator model under desert pollution," *IEEE Transactions on Dielectrics and Electrical Insulation*, vol. 25, no. 6, pp. 2296–2304, 2018.

[17] N. Dhahbi-Megriche and A. Beroual, "Time–frequency analyses of leakage current waveforms of high voltage insulators in uniform and non-uniform polluted conditions," *IET Science, Measurement & Technology*, vol. 9, no. 8, pp. 945–954, 2015.

[18] M. F. Palangar and M. Mirzaie, "Diagnosis of porcelain and glass insulators conditions using phase angle index based on experimental tests," *IEEE Transactions on Dielectrics and Electrical Insulation*, vol. 23, no. 3, pp. 1460–1466, 2016.

[19] D. Fauziah, H. Alfiadi *et al.*, "The effect of coating on leakage current characteristic of coast field aged ceramic insulator," in *2017 4th International Conference on Electrical Engineering, Computer Science and Informatics (EECSI)*. IEEE, 2017, pp. 1–7.

[20] M. E. Ibrahim and A. M. Abd-Elhady, "Rogowski coil transducer-based condition monitoring of high voltage insulators," *IEEE Sensors Journal*, vol. 20, no. 22, pp. 13 694–13 703, 2020.